Assimilative Modeling of Ionospheric Dynamics for Now-casting of HF Propagation Channels in the Presence of TIDs[1]

L. J. Nickisch, Sergey Fridman, Mark Hausman, Shawn Kraut, George Zunich*
NorthWest Research Associates, 301 Webster St., Monterey, CA 93940
*Zunicalc, Inc.

The ionospheric data assimilation algorithm called GPS Ionospheric Inversion (GPSII; pronounced "gypsy") [*Fridman et al.*, 2006, 2012; *McNamara et al.*, 2013] has been extended and employed to model the dynamic ionosphere, including medium-scale traveling ionospheric disturbances (MS-TIDs). GPSII can assimilate many forms of ionospheric-related data, including ionogram data and GPS L1/L2 beacon data. For this effort, GPSII was extended to assimilate delay, Doppler, and angle-of-arrival (AoA) measurements of HF transmissions from known reference points (KRPs). A companion paper [*Fridman, et al.*, 2015; these proceedings] documents the development of the assimilation capability for KRPs. In this paper we show test results of the model's performance in reproducing measured AoA variations in the presence of medium-scale traveling ionospheric disturbances (MS-TIDs) using Near Vertical Incidence Skywave (NVIS) data collected at White Sands Missile Range by the IARPA HFGeo Program Government team. We find, using three KRPs within approximately 50 km of non-assimilated transmitters, we can reproduce the measured AoAs of the non-assimilated transmitters to within 1.8 degrees with 90% confidence even in the presence of highly dynamic MS-TIDs.

1. Introduction

The primary objective of this work, sponsored by the IARPA HFGeo program[1], is to model the dynamic ionosphere, including ionospheric perturbations such as traveling ionospheric disturbances (TIDs), to support improved HF geolocation accuracy. The approach adopted by the NorthWest Research Associates (NWRA) team is to use the technique of ionospheric data assimilation to model the three-dimensional electron density distribution of the ionosphere. NWRA's ionospheric data assimilation algorithm, called GPS Ionospheric Inversion (GPSII; pronounced "gypsy") has been augmented and employed for this task [*Fridman et al.*, 2006, 2009; *McNamara et al.*, 2013]. GPSII can assimilate many forms of ionospheric-related data, including ionogram data and GPS L1/L2 beacon data. For this effort, GPSII was extended to assimilate delay-Doppler data of HF transmissions from known reference points (KRPs). We also improved GPSII's ability to assimilate measured angles-of-arrival (AoAs) of KRPs. The companion paper [*Fridman, et al.*, 2015] documents the development of the assimilation capability for KRPs.

The paper is organized as follows. In Section 2 we describe the link geometries and array configuration for the data collections. In Section 3 we show comparisons of measured AoAs and computed AoAs from numerical ray tracing in the ionosphere model generated by GPSII when assimilating only delay-Doppler data. Section 4 shows similar comparisons, but for assimilation of delay-Doppler data plus AoA data from three links as well as a vertical ionogram. Concluding remarks are made in Section 5.

2. HF NVIS Link Geometry

The methodology we have employed involves ionospheric modeling through data assimilation using GPSII, then numerically ray tracing through the derived ionosphere model to predict angles-of-arrival, slant

[1] This research is based upon work supported in part by the Office of the Director of National Intelligence (ODNI) Intelligence Advanced Research Projects Activity (IARPA) HFGeo program under contract 2013-13082600004. The views and conclusions contained herein are those of the authors and should not be interpreted as necessarily representing the official policies or endorsements, either expressed or implied, of ODNI, IARPA, or the U.S. Government. The U.S. Government is authorized to reproduce and distribute reprints for Governmental purposes notwithstanding any copyright annotation thereon.

range (time delay times the speed of light), and Doppler shift for test links for comparison to Government estimates of the same. The Government estimates of AoA were obtained using a hexagonal array of nineteen pairs of crossed dipoles, as shown in Figure 1. Our analysis presented here utilizes KRP data with transmission frequency 5.3 MHz.

The NWRA team was provided with samples of data from the Government collection of January 2014 at White Sands Missile Range (WSMR). Many NVIS HF links within or in the vicinity of WSMR were instrumented, and AoAs were estimated at a site called G10 near the southern end of WSMR. These transmitter and receiver locations are shown in Figure 2. We will show predicted AoA results for two scenarios, 1.) delay-Doppler assimilation and 2.) delay-Doppler-AoA-ionogram assimilation. Figure 2 shows the sets of links whose data were assimilated in the two scenarios. The colored circles indicate the approximate midpath ionospheric reflection point for the assimilated links. Because of space limitations here, we can only show a limited number of cases. Complete results are available in *Nickisch, et al.* [2014].

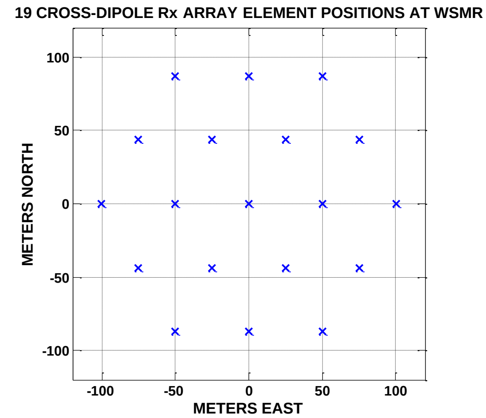

Figure 1. Geometry of crossed dipole array at site G10 used for AoA measurements.

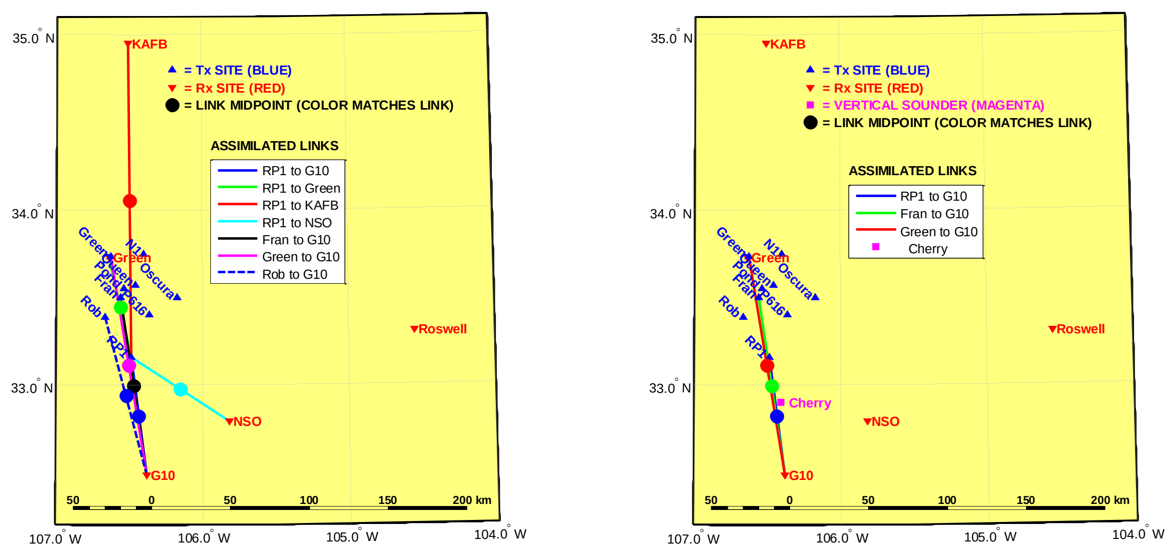

Figure 2. Transmitters and receiver locations for the WSMR campaign. Left: Map of link geometries whose delay-Doppler time histories were assimilated for the predicted AoA results shown in Section 3. Right: Map of link geometries whose delay-Doppler-AoA time histories were assimilated for the results shown in Sections 4, plus location of vertical Digisonde at Cherry.

3. Delay-Doppler Assimilation

The GPSII ionospheric data assimilation algorithm allows testing for a number of types of ionospheric-related input data. In this section we show that ingesting delay and Doppler data alone from known reference transmitters is sufficient to predict angle-of-arrival variations caused by MS-TIDs – without directly assimilating any AoA data or ionogram data. To our knowledge, this is the first time in the history of

HF propagation modeling that this has ever been accomplished. In the section following this one, we will show that AoA assimilation from KRPs further improves the ability to predict AoA of non-assimilated links.

The next set of figures show examples of GPSII predictions compared to the Government-provided estimates of AoA for data collected on the WSMR campaign on 19 January 2014. Figure 3 shows results for a link whose delay-Doppler time series data were assimilated into GPSII to estimate the 3D ionosphere (the full set of assimilated links is shown in the left pane of Figure 2). In the panes on the left side of Figure 3, it is clear to the eye that the GPSII model is capturing the temporal behavior of the medium-scale TIDs very well. The pane on the upper right shows a scatter plot of the differences between the Government-provided estimates and the GPSII prediction, and on the lower right is the cumulative distribution function (CDF) of the differences, plotted as circular errors in milli-steradians (mSR) – that is, $2\pi(1-\cos(\Delta\theta))$ where $\Delta\theta$ is the cone angle between the estimate and the prediction. It is convenient to note that $\Delta\theta(\text{deg}) \approx (\text{circular error in mSR})^{1/2}$, so 2 mSR corresponds to a cone angle of about 1.4°. The AoA predictions for the other assimilated links received at G10 (not shown) are in just as good agreement as the one shown in Figure 3 (see *Nickisch, et al.* [2014]). Again, we point out AoA measurements themselves were not assimilated. This demonstrates that there is enough information contained in the delay-Doppler structure alone to find a 3D MS-TID-inclusive ionosphere model that is capable of manifesting the AoA fluctuations.

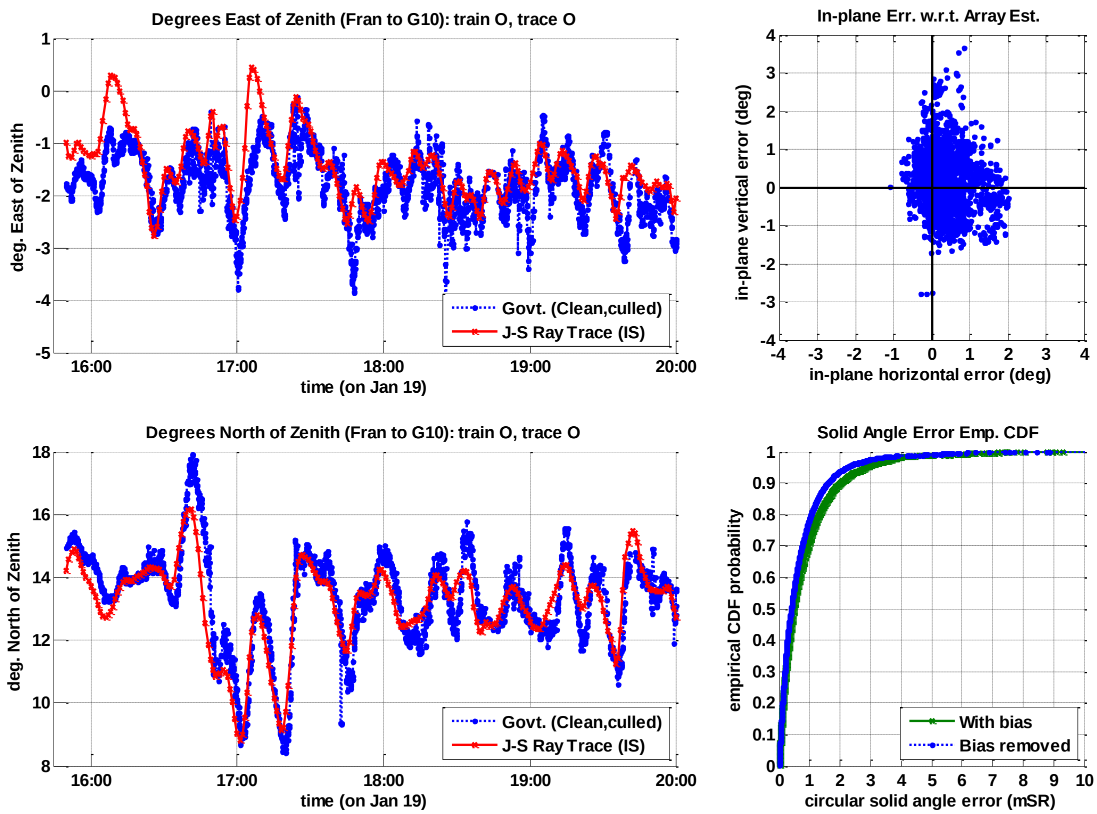

Figure 3. GPSII AoA predictions for an <u>assimilated</u> link compared to Government-provided AoA estimates for 19 JAN 2014. Only delay and Doppler data were assimilated.

The pane on the upper right shows a scatter plot of the differences between the Government-provided estimates and the GPSII predictions, and on the lower right is the cumulative distribution of the differences, plotted as circular errors in milli-steradians (mSR).

Figure 4 is similar to Figure 3, but for a link whose delay-Doppler data were <u>not</u> assimilated into the GPSII solution. Note that the AoA agreement between the Government-provided estimates and the GPSII predictions is just as good as in the case of Figure 3. The largest error all other non-assimilated links (not shown; see *Nickisch, et al.* [2014]) was a circular error 3.5 mSR at the 90^{th} percentile level, corresponding to a 1.9° miss. This was for the southernmost link, and the increase in error for this link is due to the ionospheric model "anticipating" the TID perturbations a couple of minutes early. This appears to be occurring because GPSII, currently, is assimilating data without knowledge of how the TIDs are propagating. Most of the ionospheric sampling points are to the north and, in this case, the TID is progressing toward the south. Hence GPSII is applying the TID modifications a little temporally early to this southerly link. We expect this effect to be reduced when the GPSII algorithm is extended to account for knowledge of TID propagation physics in our ongoing work.

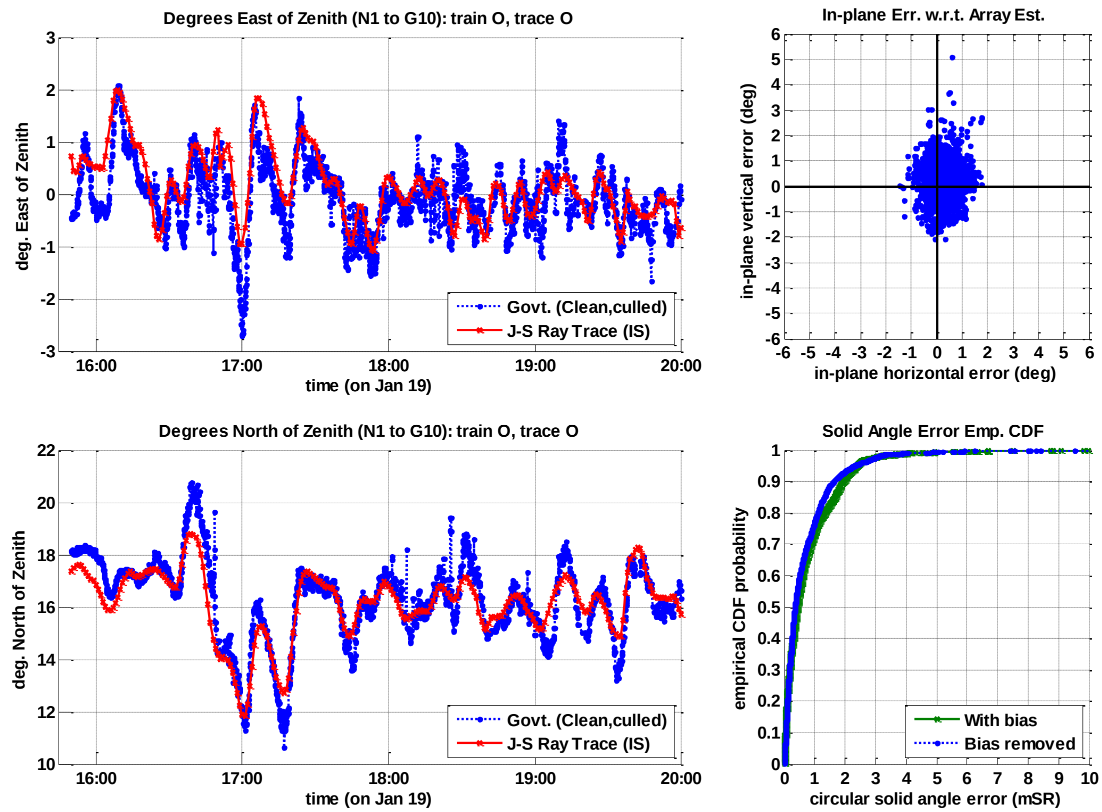

Figure 4. GPSII AoA predictions for a <u>non-assimilated</u> link compared to Government-provided AoA estimates for 19 JAN 2014. (Note: Assimilated links only used delay-Doppler data. No AoA or ionogram data were assimilated.)

4. Delay-Doppler-AoA-ionogram assimilation

In this section we show results for the assimilation of delay-Doppler-AoA data, plus we also assimilated data from the vertical sounder at the location named Cherry within WSMR. The assimilated links and the sounder location are shown in the right pane of Figure 2. Note that the assimilated links are reduced to three in number, all received at the common location G10. Note also that the three links are essentially collinear. As we show below, the lack of cross-range diversity did not seem to cause significant degradation after the first half-hour or so of the assimilation, presumably due to the traveling nature of the TIDs that, over time, effectively provides the algorithm with some cross-range information.

Figure 5 through Figure 8 are again for 19 January 2014. Figure 5 shows AoA results for one of the three assimilated links. The result for this and the other two assimilated links (not shown) are very good. Figure 6 shows the AoA results for a non-assimilated link, and the CDF shows the circular error crossing the 90th percentile at about 0.5 mSR, corresponding to 0.7° coning angle error. Figure 7 shows the cumulative distribution functions of circular error for the remaining <u>non-assimilated</u> links. (The Oscura link is excluded because it was only on for a short period of time, but is shown in [*Nickisch, et al.*, 2014].)

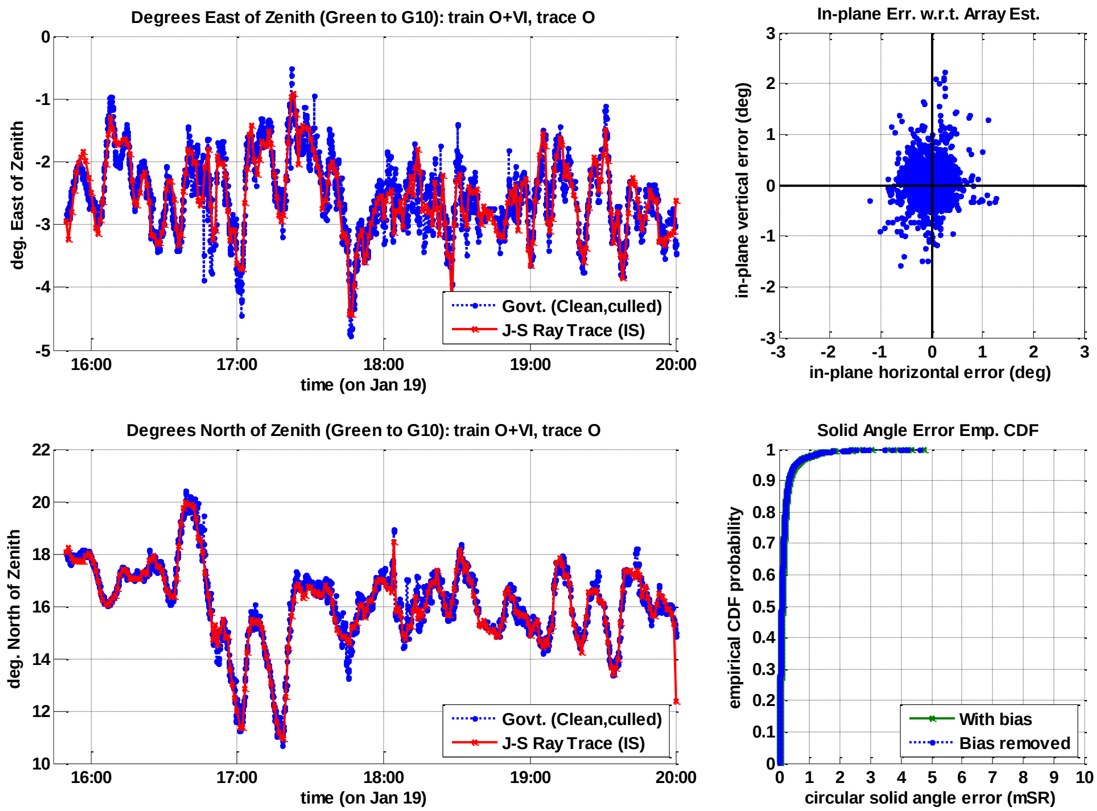

Figure 5. **GPSII AoA predictions for an <u>assimilated</u> link compared to Government AoA estimates for 19 JAN 2014. Delay-Doppler-AoA-ionogram data were assimilated.**

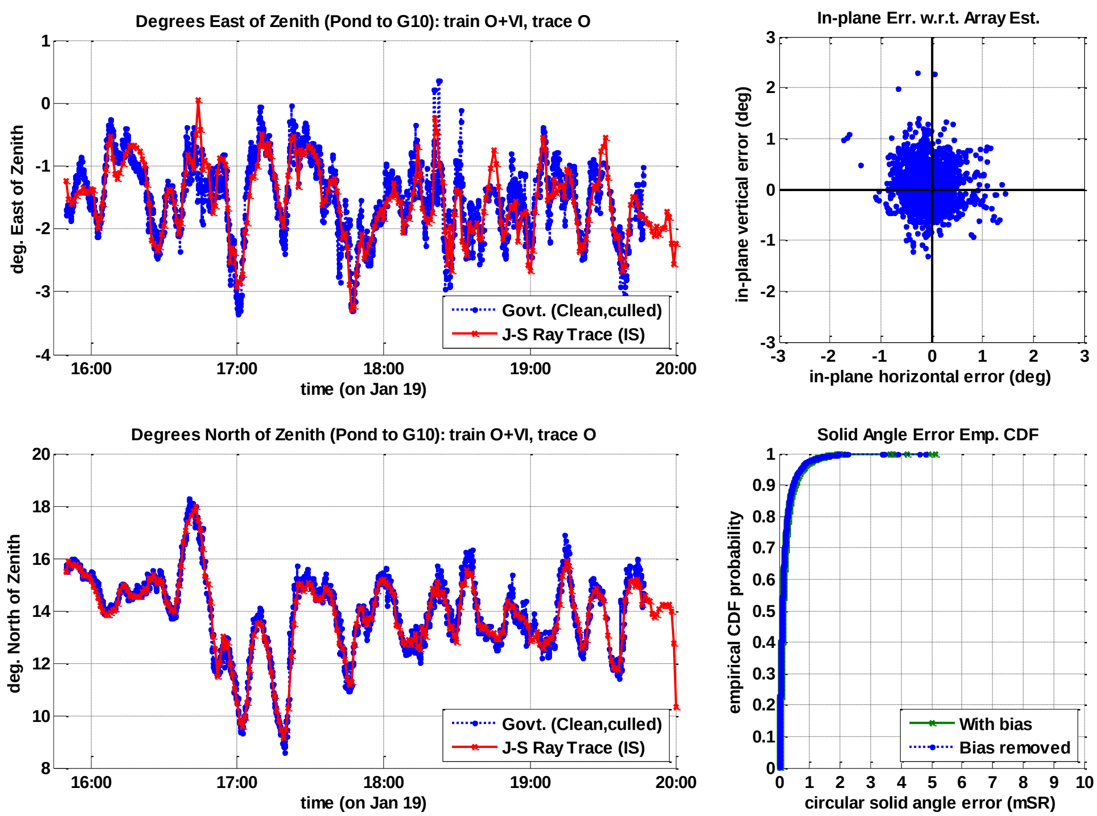

Figure 6. **GPSII AoA predictions for a <u>non-assimilated</u> link compared to Government-provided AoA estimates for 19 JAN 2014.**

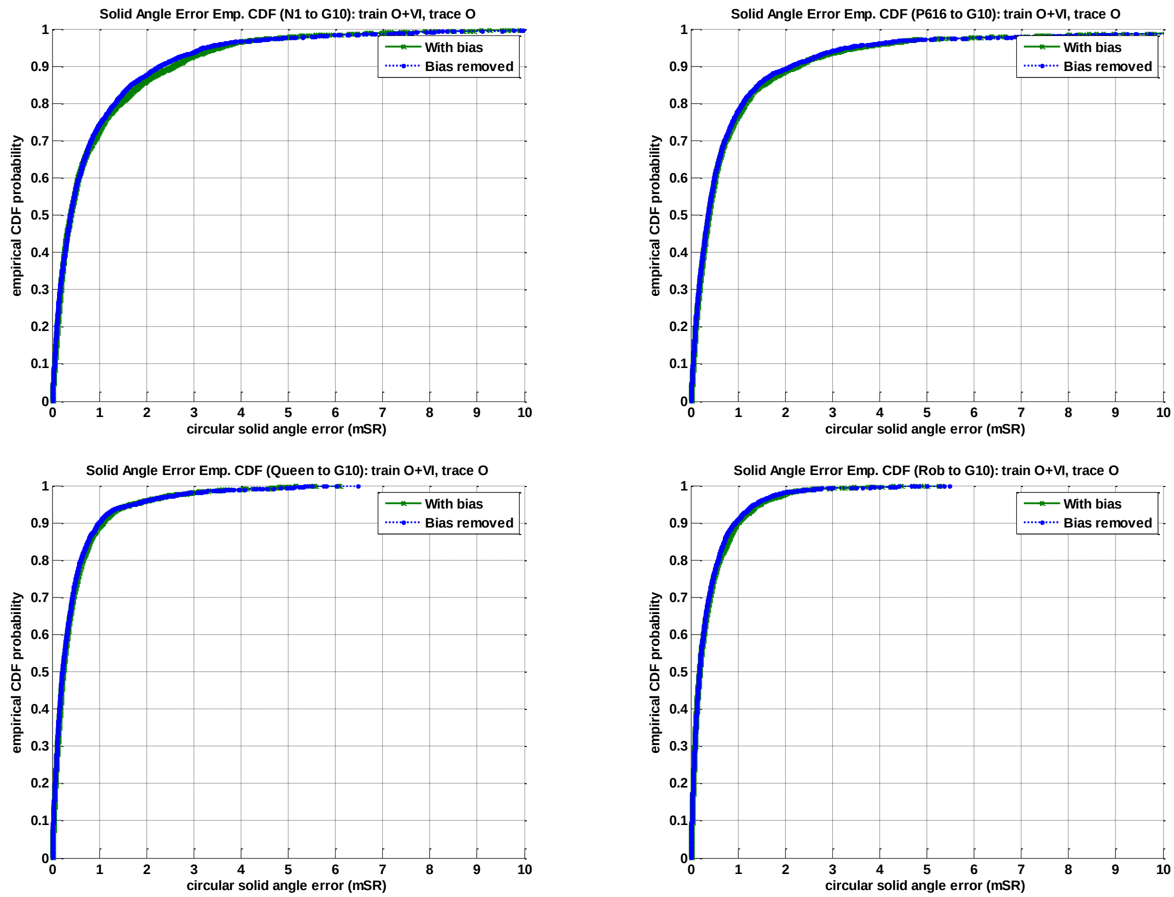

Figure 7. **Cumulative distribution functions of the differences between the Government-provided AoA estimates and the GPSII predictions for 19 JAN 2014.**
No AoA-delay-Doppler sounding data were assimilated into GPSII for these links.

In Figure 8 we compare synthetic ionograms created from the GPSII solution to those measured by the Cherry Digisonde. The ionogram information that was assimilated include the ordinary-mode (O-mode) critical frequency (foF2) and five delay-frequency pairs along the O-mode between about 5 MHz and 90% of foF2. Indeed, all of the synthesized O-mode traces match the underlying gray-scale data very well at these points. That the agreement degrades at the lower frequencies is attributable to the fact that ionogram data at these frequencies were not assimilated. We intentionally excluded these lower frequencies from the assimilation, temporarily, until we have time to address some difficulties with the F1-F2 transition region: The ionospheric F1-F2 transition region is highly dynamic and very hard to model accurately, plus there are certain modeling assumptions in IRI, GPSII's background ionosphere model that tend to cause larger F1-F2 transition cusps than these data would indicate. Such cusps are caused by a very subtle steepening of the electron density profile at the F1-F2 transition. We plan to address these issues in future work.

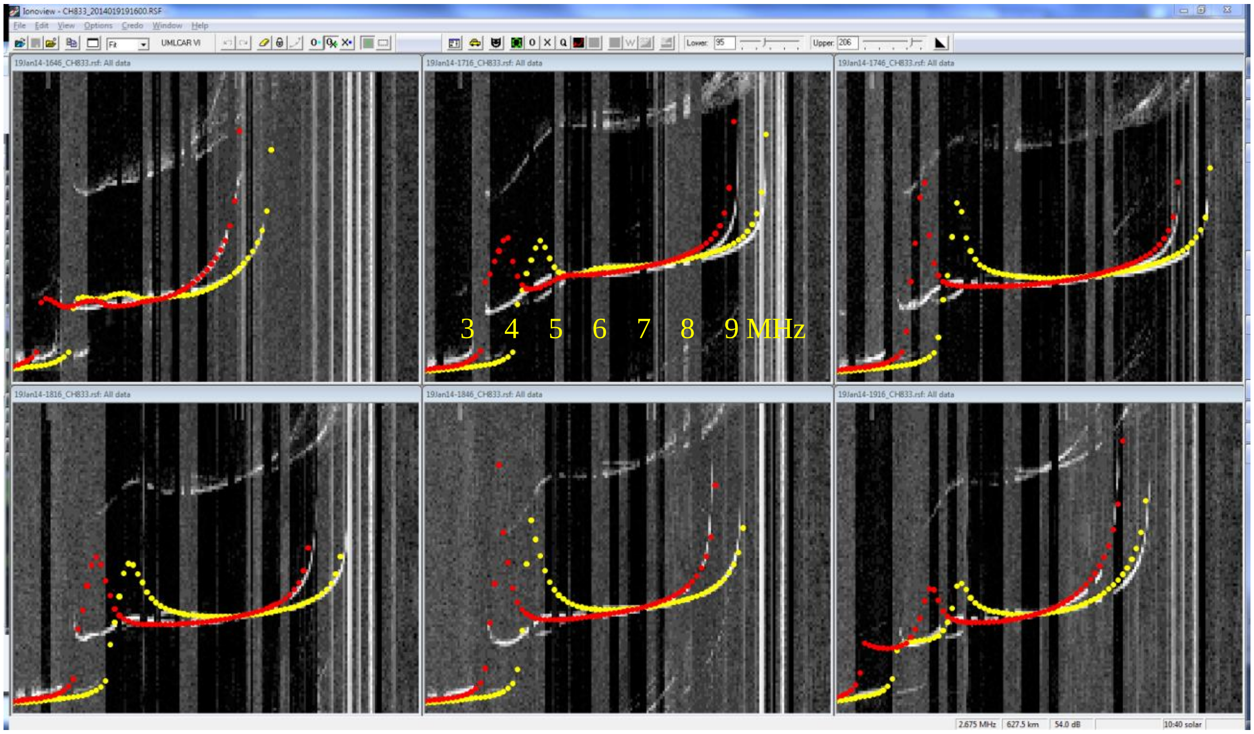

Figure 8. **GPSII synthetic ionograms (colored points) compared to Government Digisonde measurements at Cherry (grayscale image) for 19 JAN 2014. The ionograms are separated by 30 minutes.**

The scale on each of the ionograms is horizontally 2.2 to 11 MHz at 0.05 MHz resolution and vertically from 80 to 640 km at a resolution of 5 km virtual height.

The most highly disturbed TID activity provided by the Government from the WSMR campaign was on 26 January 2014. Figure 9 through Figure 11 show that even for these data, assimilation of AoA-Delay-Doppler data on the same three links (plus the ionogram at Cherry) provides very good AoA prediction results for the unassimilated links. Of the five non-assimilated links shown (Figure 10 and Figure 11), all but the N1 link have 90th percentile CDF crossings below 2 mSR circular error (1.4° cone angle error); the CDF for N1 crosses 90% at about 3.2 mSR, corresponding to 1.8° cone angle error.

In Figure 9 and Figure 10, just after 2100 UT there is a notable “glitch” on the “deg. East of Zenith” plots where the ray trace fails to follow the Government angle estimates. We have investigated this occurrence and found that during this time there are multiple modes occurring for this link reflecting from different parts of a highly distorted ionosphere, and the external ray tracing sometimes homes to the “wrong” mode (that is, a different one than was included in the Government estimates), or else does not successfully home at all (after 20 iterations, the homing algorithm ceases its attempt to home). Such occurrences are relatively rare and seem to happen only during especially rapid changes in AoA such as the time period following 2100 UT in this example.

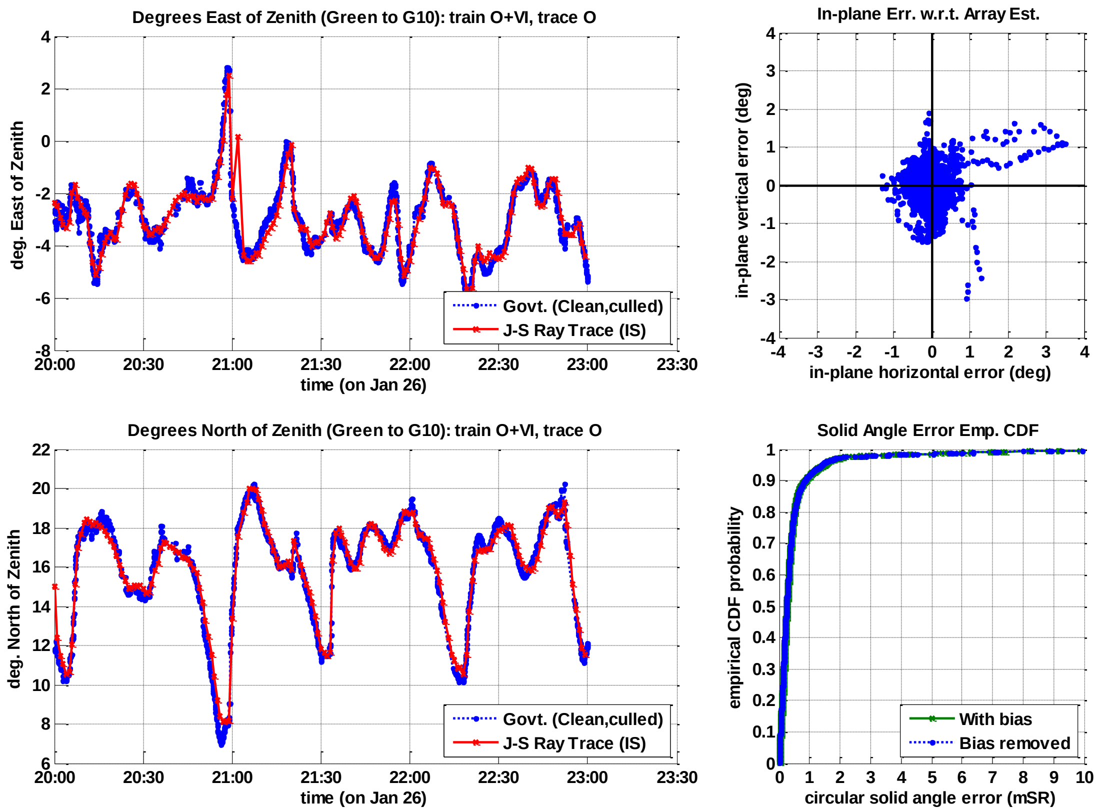

Figure 9. **GPSII AoA result for an <u>assimilated</u> link compared to Government-provided AoA estimates for 26 JAN 2014. Delay-Doppler-AoA-ionogram data were assimilated.**

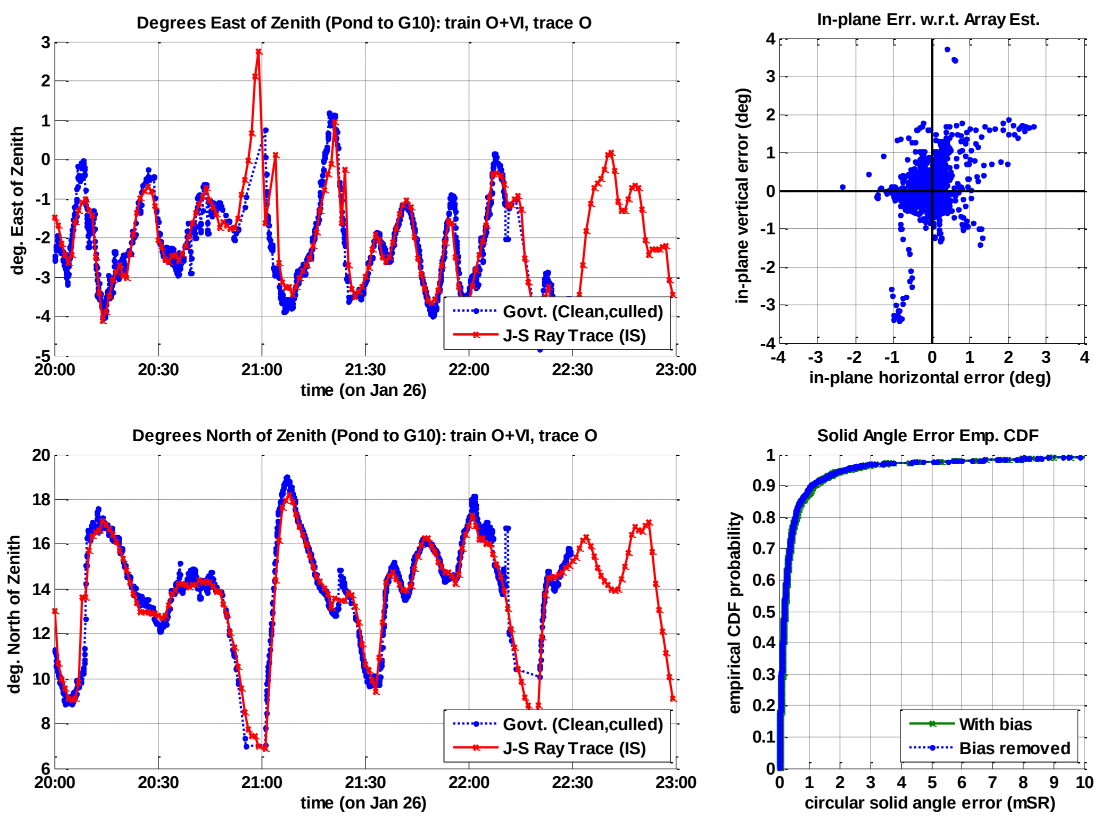

Figure 10. **GPSII AoA predictions for a <u>non-assimilated</u> link compared to Government-provided AoA estimates 26 JAN 2014.**

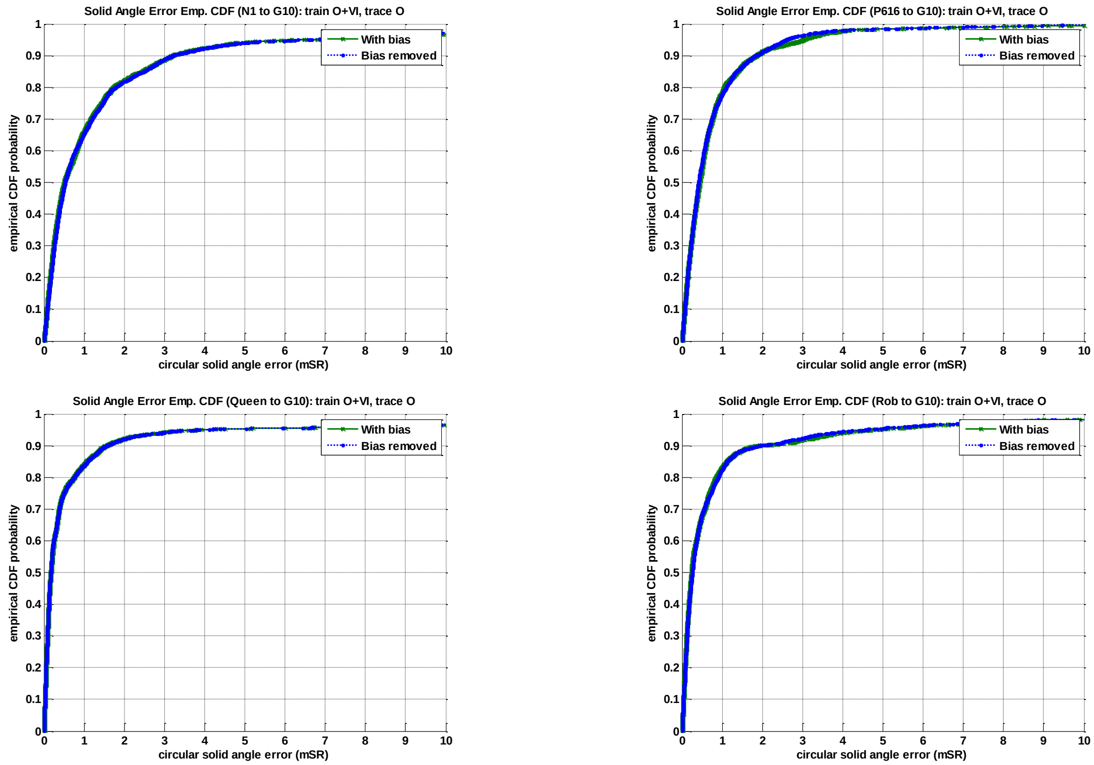

Figure 11. Cumulative distribution functions of the differences between the Government-provided estimates and the GPSII predictions 26 JAN 2014.

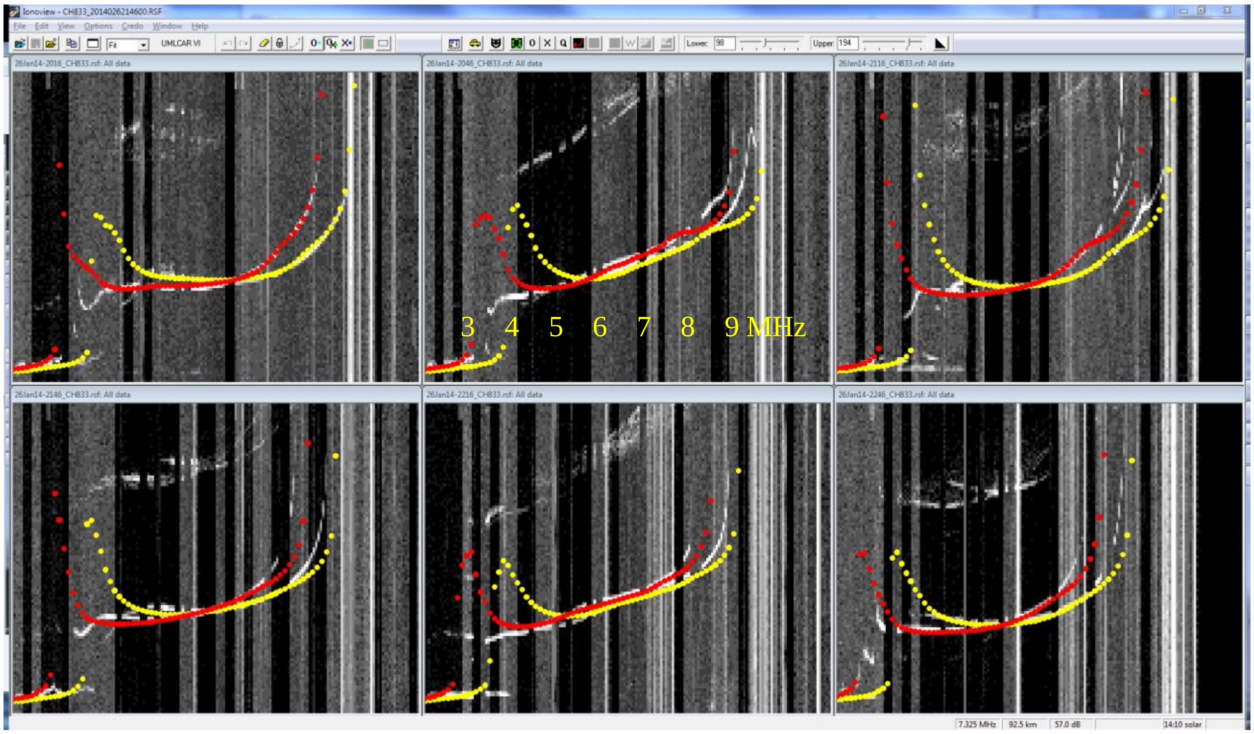

Figure 12. GPSII synthetic ionograms (colored points) compared to Government Digisonde measurements at Cherry (grayscale image) 26 JAN 2014. The ionograms are separated by 30 minutes.

The scale on each of the ionograms is horizontally 2.2 to 11 MHz at 0.05 MHz resolution and vertically from 80 to 640 km at a resolution of 5 km virtual height.

The ionograms in Figure 12 show severe TID activity, which degrades agreement slightly compared to the results shown above for the 19th. However, considering that only O-mode data between 5 MHz and 90% of the O-mode critical frequency were assimilated, along with the O-mode critical frequency, the results are for the most part in agreement at these points. The ionogram at the upper right on Figure 12 even catches the extra TID loop at the highest frequencies, though not at quite the right delay.

5. Conclusion

To our knowledge, ionospheric modeling with the fidelity to follow medium-scale TID-induced angle-of-arrival, delay, and Doppler fluctuations to the accuracies we have demonstrated has never before been attained prior the work reported here. This should be considered a major achievement of the IARPA HFGeo program.

Best results were obtained when angles-of-arrival from a small number (3) of check target signals were assimilated in GPSII (as shown in Section 4). Then, even for the strongest TID activity case (26 January 2014), it was possible to achieve 90th percentile CDF crossings of AoA error below 2 mSR (1.4° cone angle error) most of the time. (One case produced a 90% CDF crossing at 3.2 mSR, corresponding to 1.8° cone angle error.) But it is very interesting that quite good results can also be obtained even when AoA is not assimilated, as long as delay-Doppler data is assimilated for the check targets (as shown in Section 3). This shows the power of Doppler shift as a measure of TID structure and corresponding ionospheric tilts.

Not reported here, but shown in *Nickisch, et al.* [2014], we have found that the use of GNSS two-frequency beacon data degrades the fidelity of the GPSII solution for modeling medium-scale TIDs relative to AoA and/or Doppler assimilation. This is understandable because of the fact that the total electron content (TEC) of GNSS links is dominated by the topside ionosphere and plasmasphere, whereas the HF skywave signals of interest for the HFGeo program remain in the lower portion of the bottom side of the ionosphere, which accounts for only a few percent of the GNSS TEC and can be masked by measurement jitter. With modeling improvements for the topside and plasmasphere together with the incorporation of an actual TID wave model for the distribution of the TID structure in altitude, it may be possible to improve on this in the future.

References

Fridman, Sergey V., L. J. Nickisch, Mark Aiello, and Mark A. Hausman (2006), Real time reconstruction of the three-dimensional ionosphere using data from a network of GPS receivers, *Radio Sci., 41*, RS5S12, doi:10.1029/2005RS003341.

Fridman, Sergey V., L. J. Nickisch, and Mark Hausman (2012), Inversion of backscatter ionograms and TEC data for over-the-horizon radar, *Radio Sci., 47*, RS0L10, doi:10.1029/2011RS004932.

Fridman, Sergey V., L. J. Nickisch, Mark Hausman, Shawn Kraut, and George Zunich (2015), Assimilative Model for Ionospheric Dynamics Employing Delay, Doppler, and Direction of Arrival Measurements from Multiple HF Channels, 2015 Ionospheric Effects Symposium proceedings.

McNamara, L. F., M. J. Angling, S. Elvidge, S. V. Fridman, M. A. Hausman, L. J. Nickisch, and L.-A. McKinnell (2013), Assimilation procedures for updating ionospheric profiles below the F2 peak, *Radio Sci., 48*, doi:10.1002/rds.20020.

Nickisch, L. J., Sergey V. Fridman, Mark A. Hausman, Shawn Kraut, Greg Bullock, George Zunich, and Geoff Crowley (2014), Ionospheric Measurement and Modeling: IARPA HFGeo Phase 1B Interim Technical Report, Interim Technical Report for contract IARPA 2013-13082600004, NorthWest Research Associates report NWRA-14-RM550.